LETTER TO THE EDITOR

L- to H-Mode transitions at low density in ASDEX Upgrade

P. Sauter, T. Pütterich, F. Ryter, E. Viezzer, E. Wolfrum, G.D. Conway, R. Fischer, B. Kurzan, R.M. McDermott, S.K. Rathgeber and the ASDEX Upgrade Team

Max-Planck-Institut für Plasmaphysik, EURATOM Association, Garching, Germany

E-mail: pierre.sauter@ipp.mpg.de

Abstract. The results from ASDEX Upgrade discharges dedicated specifically to the investigation of low-density L-to-H transitions are presented. The plasmas were heated by ECRH to achieve a separation of electron and ion heat channels. Under such conditions, the ratio of electron to ion temperature at the plasma edge increases with decreasing density at the L-H transition and can be as high as 3.5. Our results strongly support the essential role of the ion channel in the L-H transition, via the diamagnetic E_r provided by the ion pressure gradient.

1. Introduction

The good confinement of the H-Mode, provided by an edge transport barrier, is reached above a certain power threshold P_{thres}, which increases with plasma density and magnetic field, $P_{\mathrm{thres}} \approx \bar{n}_e^{0.72} B_T^{0.80}$, as yielded by scaling expressions, see e.g [1]. However, the scalings are only valid above a certain density, $\bar{n}_{e,\mathrm{min}}$, which depends on device and plasma conditions [1]. Below $\bar{n}_{e,\mathrm{min}}$, in the "low-density branch", P_{thres} also increases as $\bar{n}_e$ decreases, as observed in several devices, [2, 3, 4, 5, 6, 7]. At ASDEX Upgrade $\bar{n}_{e,\mathrm{min}}$ is around $4 \times 10^{19}\,\mathrm{m}^{-3}$, as shown in [8]. The discharges performed for the present work confirm the previous results and extend the density range down to $\bar{n}_e \approx 1.5 \times 10^{19}\,\mathrm{m}^{-3}$ (Fig. 1). So far, this behavior has not been definitely assigned to a physics mechanism. Experimental results from JET suggest that a fixed edge ion temperature might be required at the L-H transition [9]. Previous studies in various devices generally implied that an edge T_e threshold might be the condition for the L-H transition [5, 4]. Indeed, the role of the electron and ion channels in the L-H transition physics is not identified. It can only be investigated under plasma conditions allowing a separation of the channels, which implies low density and dominant heating into one of the two channels. In ASDEX Upgrade, this question has been addressed by applying Electron Cyclotron Resonance Heating (ECRH) in the low-density branch of P_{thres}, and indeed a clear separation of the two channels at the L-H transition could be achieved.

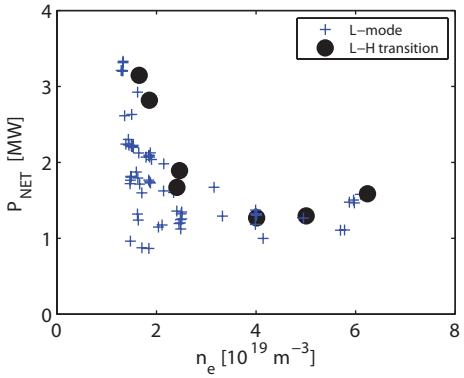

Figure 1: Power threshold versus line averaged density for the investigated data set

2. Experiments and profile analysis

The study was conducted in deuterium plasma, in a standard lower single null configuration, which corresponds to the favorable ion ∇B drift for P_{thres}. The plasma

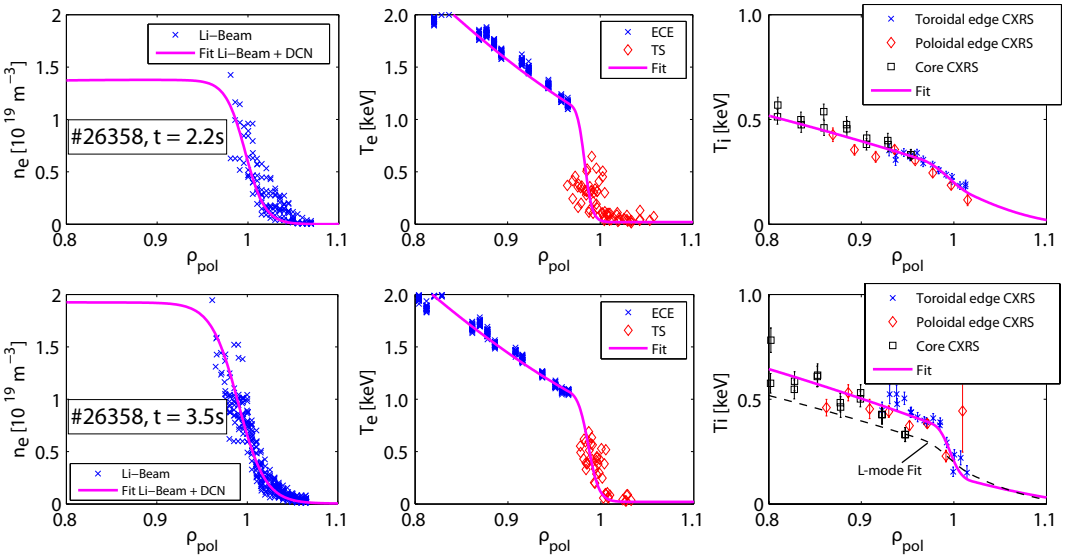

Figure 2: Fitted edge profiles; upper row high power L-Mode; lower row H-Mode

current was 1 MA and the magnetic field $B_T = -2.3$ T, yielding $q_{95} \approx 4$. The ECRH power was deposited in the plasma center and absorbed by the electrons with nearly 100% efficiency in a very narrow deposition profile (width ≈ 3 cm), as yielded by the beam tracing code TORBEAM [10]. The discharges were generally carried out by increasing the ECRH power at fixed density, following the path from L-Mode to H-Mode. At densities below $n_{e,\min}$, however, it is also possible to increase the density at constant heating power, crossing the L-H transition at a given density. Both methods yield the same results. The L-H transition is generally preceded by an intermediate limit-cycle phase, in which the plasma oscillates between high and low confinement, described in detail in [11] and labeled I-phase.

The electron temperature, T_e, is measured with an electron cyclotron emission (ECE) radiometer with 60 radial channels yielding a spatial resolution as low as 1 cm in the edge region with a sampling rate of 31.25 kHz. This diagnostic requires sufficient optical thickness to yield the correct temperature, which is not always fulfilled at the very edge in our discharges. Such measurement points have been identified and discarded. Therefore, our edge Thomson scattering (TS), which yields 16 radial points around the separatrix with a spatial resolution in the millimeter range, is essential to assess the T_e profiles, by combining the two diagnostics.

The edge density is measured with the Lithium-beam diagnostic, [12], which delivers electron density measurements with a spatial resolution of 5 mm and a sub-millisecond temporal resolution. This measurement is combined with the far-infrared laser interferometry system to provide the complete density profile.

The measurement of the edge ion temperature T_i is essential for our study. It is provided by 2 recently installed edge systems, with poloidal and toroidal views, and one core system, all three based on the usual Charge Exchange Recombination Spectroscopy on impurities. Both edge systems [13] each consist of 8 lines of sight. Their spatial resolution is about 1 cm with a time resolution around 2 ms. The CXRS measurement in our discharges is provided by 8 ms long blips of the required Neutral Injection Beam (NBI) with a power of about 1.5 MW repeated every 100 ms. This has proven sufficient to get enough light for the analysis. The slowing-down time of the fast ions resulting from NBI is much longer than the T_i measurement which is therefore not affected by the blip heat pulse.

Examples of edge density and temperature profiles in L-Mode just before the oscillation phase, and H-Mode just after the transition are shown in Fig. 2. This was AUG dis-

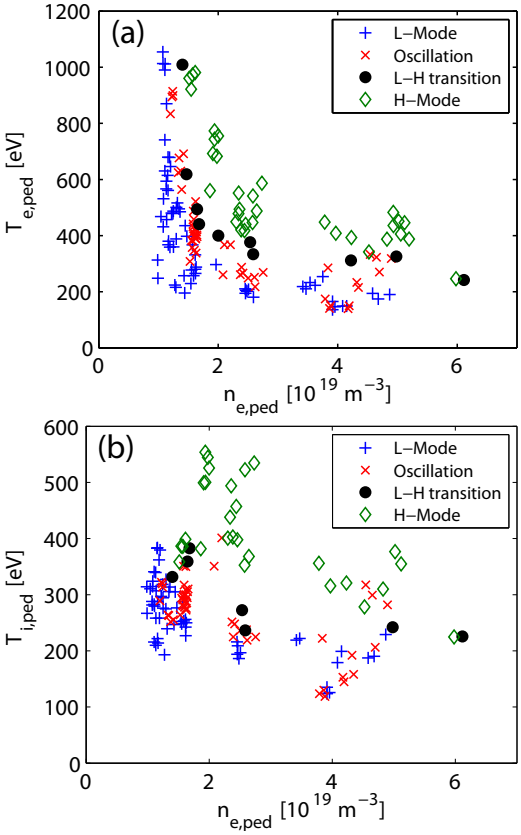

Figure 3: Pedestal values of (a) T_e and (b) T_i versus $n_{e,\mathrm{ped}}$ for the different regimes

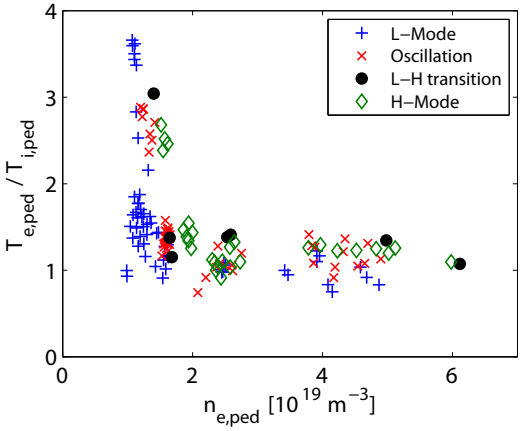

Figure 4: Ratio of electron and ion edge temperature

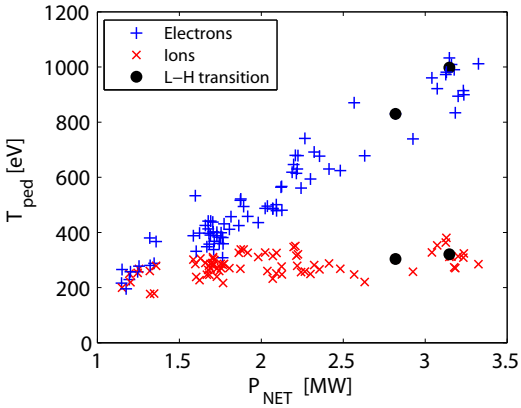

Figure 5: Separation of electron and ion edge temperature at a fixed pedestal density around $1.4 \pm 0.25 \times 10^{19}\,\mathrm{m}^{-3}$

charge #26358, with ECRH power of about 3 MW and a slight increase of density to reach the L-H transition. The data points are shown together with a fit using a modified hyperbolic tangent function, [14], from which we derive position and value of the pedestal top, as well as the gradient. For cases where the pedestal is not visible in the L-Mode, its position determined in the following H-Mode phase is used to extract the L-Mode data. A pronounced pedestal in T_e with a value $T_{e,\mathrm{ped}} \approx 1$ keV at the top is visible in the L-Mode. This is a general feature of our low density L-Modes with strong ECRH in which $T_{e,\mathrm{ped}}$ increases with heating power, as will be shown below. The measured density pedestal in L-Mode is a widely observed feature (e.g. [15, 16]). In contrast, T_i exhibits a very weak pedestal: its value at the radial position of $T_{e,\mathrm{ped}}$ reaches about 0.3 keV, 3 times lower than $T_{e,\mathrm{ped}}$. The edge T_i gradient is low. In the H-Mode, Fig. 2 lower row, a clear pedestal in T_i appears, as usually observed in this regime, while T_e is almost unchanged. However $T_{e,\mathrm{ped}}$ remains much higher than $T_{i,\mathrm{ped}}$. The density is about 20% higher, but retains the same profile shape.

Transport analyses, which are out of the scope of this work, indicate that the strong T_e gradient, present already in L-Mode and unaffected by the L-H transition, is caused by an edge transport barrier for electron heat in the L-Mode. This feature becomes particularly visible under conditions of high heating power without entering the H-Mode, i.e. high P_{thres}, and is very similar to the so called I-mode, which also requires high P_{thres} conditions [17, 18].

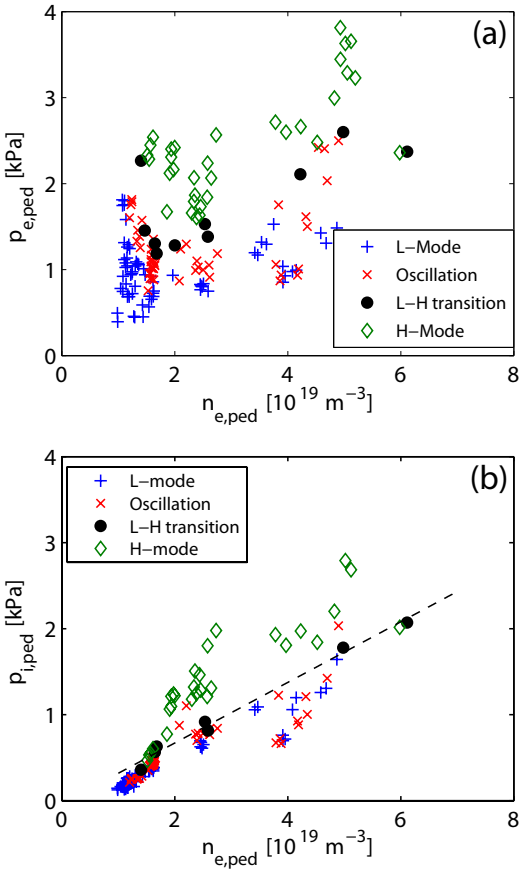

Figure 6: (a) Electron and (b) ion pedestal top pressure

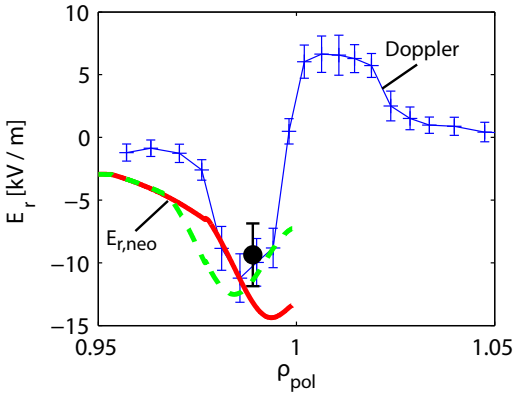

Figure 7: Comparison of E_r in oscillation phases: Doppler Reflectometry profile (#24812, 2.7s) and single point (#24906, 2.3s, circle), $E_{r,\mathrm{neo}}$ (#24906, 2.3s, solid) and effect of shifting T_i by 0.01 in ρ_{pol} (dashed)

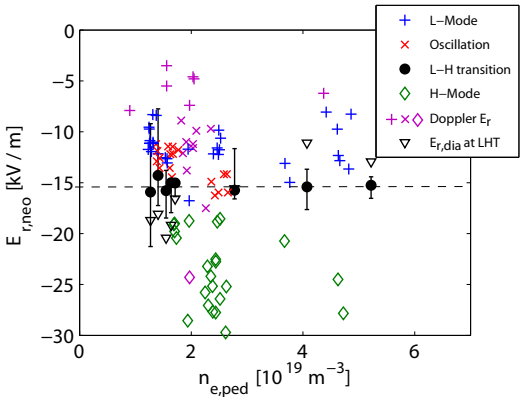

Figure 8: $E_{r,\mathrm{neo}}$ versus $n_{e,\mathrm{ped}}$, Doppler E_r and $E_{r,\mathrm{dia}}$ for L-H transitions only (always minimum values)

3. Overview of the pedestal results

Such analyses have been carried out for several discharges at different densities yielding data for L-Mode, oscillation and H-Mode phases, as well as just before the L-H transition. The results are shown in Fig. 3 where the dependence of $T_{e,\mathrm{ped}}$ and $T_{i,\mathrm{ped}}$ are plotted versus the corresponding pedestal top of density $n_{e,\mathrm{ped}}$. The values of $T_{e,\mathrm{ped}}$ at the L-H transition rise steeply towards low densities, nearly increasing 5-fold in the covered range. It should be pointed out that the weak dependence of $T_{e,\mathrm{ped}}$ upon $n_{e,\mathrm{ped}}$ at the L-H transition reported for ASDEX Upgrade in [19] was deduced from a density range corresponding to $n_{e,\mathrm{ped}} > 2.5 \times 10^{19}\,\mathrm{m}^{-3}$ and therefore did not cover the low-density window where T_e strongly increases. In contrast to $T_{e,\mathrm{ped}}$, $T_{i,\mathrm{ped}}$ exhibits a moderate change by at most a factor of 2. Furthermore, as indicated by Fig. 3, both temperatures are higher in the H-Mode than in the other phases. The points corresponding to the oscillating phases are below but close to the L-H data. The L-Mode data extend from the lower boundary set by Ohmic heating up to the oscillation or L-H transition. This excursion is much larger at low density where P_{thres} is high and the separation can be well investigated.

Indeed, the ratio $T_{e,\mathrm{ped}}/T_{i,\mathrm{ped}}$ varies by a large amount versus density as illustrated in Fig. 4. The separation between electron and ion channels, reflected by the large values of $T_{e,\mathrm{ped}}/T_{i,\mathrm{ped}}$ is very clear at low densities. It begins to increase for decreasing $n_{e,\mathrm{ped}}$ below $n_{e,\mathrm{ped}} \approx 2 \times 10^{19}\,\mathrm{m}^{-3}$, which corresponds approximately to the minimum

in $P_{\rm thres}$ at $\bar{n}_e \approx 4 \times 10^{19}\,{\rm m}^{-3}$ core line averaged density.

The separation of T_e and T_i with increasing heating power at fixed density is illustrated in Fig. 5. For low heating, $P_{NET} < 1.5\,{\rm MW}$, electrons and ions are at the same temperature, but separate clearly when the power is ramped up: $T_{e,\rm ped}$ increases almost linearly while $T_{i,\rm ped}$ saturates.

Electron and ion edge pressure profiles have been calculated. The ion density has been calculated from the electron density including a dilution correction derived from density dependent $Z_{\rm eff}$ data. The experiments have been carried out in boronized wall conditions, the dominant impurities in these circumstances are Helium ($< 5\%$), Boron ($< 1\%$) and Carbon ($< 1\%$). $Z_{\rm eff}$ ranges from 1.4 at $n_{e,\rm ped} = 6 \times 10^{19}\,{\rm m}^{-3}$ up to 5 at $n_{e,\rm ped} = 1 \times 10^{19}\,{\rm m}^{-3}$. The pedestal pressure values are plotted versus $n_{e,\rm ped}$ in figure 6. For the L-H transition points, the variation of $p_{e,\rm ped}$ with density is weak, less than a factor of two, and a turn-around is observed towards low density. This behavior is significant and due to the very strong increase of T_e at very low densities, see Fig. 3. In fact, $p_{e,\rm ped}$ at the L-H transition is the local edge parameter that most resembles the global power threshold curve [8]. In contrast, $p_{i,\rm ped}$ at the L-H transition increases approximately linearly by a factor of about 4 over the covered range of $n_{e,\rm ped}$. It should be underlined that $P_{\rm thres}$ does not increase linearly with density, but that the heat flux in the ion channel might increase monotonically.

On ASDEX Upgrade, measurements of the E_r profile are possible with the Doppler Reflectometry system [20] and the installed toroidal and poloidal edge CXRS systems via the radial force balance of the observed impurity ion. However these diagnostics are not available for the whole set of discharges analyzed in this work and we therefore evaluated the diamagnetic contribution of the ion pressure gradient, given by $E_{r,\rm dia} = \frac{\nabla p_i}{Z e n_e}$ assuming $\nabla Z_{\rm eff} = 0$ in the range $\rho_{\rm pol} = 0.98 - 1.00$. The neoclassical calculation of E_r [21] consists of the diamagnetic term $E_{r,\rm dia}$ and a term which is proportional to ∇T_i, with a collisionality dependence factor α ($E_{r,\rm neo} = E_{r,\rm dia} - \alpha \nabla T_i$). In fig. 7 a Doppler Reflectometry E_r profile and $E_{r,\rm neo}$ for a typical phase prior to an L-H transition is given. The largest uncertainty in the calculation of the ion pressure gradient is stemming from the alignment of T_i and n_e profiles through the plasma equilibrium reconstruction. We have assessed its magnitude by shifting the T_i profile by ± 0.01 in $\rho_{\rm pol}$ against n_e, an example for this is also shown in fig. 7. It has to be noted that $E_{r,\rm neo}$ does not include fluid or Reynolds stress components and thus likely constitutes only a lower limit for E_r.

Fig. 8 shows the minimum of $E_{r,\rm neo}$ for the different phases at varying densities. Error bars derived from shifting the T_i profile are given for the L-H transition points. At the L-H transition $E_{r,\rm neo}$ shows no dependence on $n_{e,\rm ped}$. Included in fig. 8 are also E_r minimum values derived from Doppler Reflectometry for a different set of discharges with comparable parameters. This shows a good agreement between the two methods for the different discharge mode regimes. The very weak variation of the L-H points in $E_{r,\rm neo}$ is remarkable and underlines the possible key role of E_r in the L-H threshold.

4. Conclusions

By choosing low density and dominant electron channel heating a strong decoupling of edge T_e and T_i at the L-H transition was achieved. The results of edge profile analysis point towards the ion pressure gradient as a main player in the H-Mode transition mechanism, while for the electrons a direct role is not observable.

Recent progress in edge turbulence analysis [11, 22] suggest that both edge turbulence and a mean flow shear must be present in sufficient size to start the self-driving bootstrap process that creates the strong E_r well found in the edge of the fully developed H-Mode. Our findings complement these results, indicating that the E_r well has to reach a threshold to permit the H-Mode transition.

The strong increase of the global transition power threshold curve at low densities is caused by the decoupling of electron and ion heat flux. One may speculate that the transition to H-Mode requires a sufficiently high edge ion heat flux the reach the necessary E_r value.

References

[1] Martin Y.R. *et al.*, 2008 *Journal of Physics: Conference Series* **123** 012033 (11pp)
[2] Snipes J. *et al.*, 1996 *Nuclear Fusion* **36**(9) 1217
[3] Fielding S.J. *et al.*, 1996 *Plasma Physics and Controlled Fusion* **38**(8) 1091
[4] Hubbard A.E. *et al.*, 1998 *Plasma Physics and Controlled Fusion* **40**(5) 689
[5] Carlstrom T.N. and Groebner R.J., 1996 *Physics of Plasmas* **3**(5) 1867
[6] Fukuda T. *et al.*, 1997 *Nuclear Fusion* **37**(9) 1199
[7] Andrew Y. *et al.*, 2006 *Plasma Physics and Controlled Fusion* **48**(4) 479
[8] Ryter F. *et al.*, 2009 *Nuclear Fusion* **49**(6) 062003
[9] Andrew Y. *et al.*, 2004 *Plasma Physics and Controlled Fusion* **46**(5A) A87
[10] Poli E. *et al.*, 2001 *Computer Physics Communications* **136**(1-2) 90
[11] Conway G.D. *et al.*, 2011 *Phys. Rev. Lett.* **106**(6) 065001
[12] Fischer R. *et al.*, 2008 *Plasma Physics and Controlled Fusion* **50**(8) 085009
[13] Pütterich T. *et al.*, 2008 *Europhysics Conference Abstracts, Proceedings of the 35th EPS Conf. on Plasma Phys., CD-ROM, Vol. 32D, pp. P-2.083*
[14] Groebner R.J. and Carlstrom T.N., 1998 *Plasma Physics and Controlled Fusion* **40**(5) 673
[15] Groebner R.J. *et al.*, 2002 *Plasma Physics and Controlled Fusion* **44**(5A) A265
[16] Hughes J. *et al.*, 2007 *Nuclear Fusion* **47**(8) 1057
[17] Ryter F. *et al.*, 1998 *Plasma Physics and Controlled Fusion* **40**(5) 725
[18] Whyte D.G. *et al.*, 2010 *Nuclear Fusion* **50**(10) 105005
[19] Suttrop W. *et al.*, 1997 *Plasma Physics and Controlled Fusion* **39**(12) 2051
[20] Conway G.D. *et al.*, 2004 *Plasma Physics and Controlled Fusion* **46**(6) 951
[21] Hinton F.L. and Hazeltine R.D., 1976 *Rev. Mod. Phys.* **48**(2) 239
[22] Estrada T. *et al.*, 2010 *EPL (Europhysics Letters)* **92**(3) 35001